ISSN: 2834-7706

Research Article

Journal of Mathematical Techniques and Computational Mathematics

Quasi-Resonant Tunneling States in Triangular Double-Barrier Nanostructures

A.M. Elabsy[1*] and M.T. Attia[2]

[*]Theoretical Solid State Physics Group (TSSPG), Department of Physics, Faculty of Science, Mansoura University, P.N. 35516, Mansoura, Egypt.

[*]Corresponding Author
A. M. Elabsy, Theoretical Solid State Physics Group (TSSPG), Department of Physics, Faculty of Science, Mansoura University, P.N. 35516, Mansoura, Egypt.

Submitted: 2023, June 29; **Accepted:** 2023, July 15; **Published:** 2023, Aug 04

Citation: Elabsy, A. M., Attia, M. T. (2023). Quasi-Resonant Tunneling States in Triangular Double-Barrier Nanostructures. *J Math Techniques Comput Math, 2*(8), 347-355.

Abstract

The quasi-resonant tunneling energies and lifetimes of symmetrical triangular double-barrier nanostructures fabricated from GaAs-Al$_y$Ga$_{1-y}$As were investigated. The complex energy approach is used to calculate the resonant tunneling energy and its associated lifetime. The results show that decreasing the well width and increasing the aluminum concentration within the barrier material enhances the quasi-resonant tunneling energies for a fixed barrier thickness. Furthermore, increasing both the aluminum concentration and the barrier thickness results in longer resonant tunneling lifetimes. The current study's findings show that resonant tunneling energies and lifetimes closely match available data in the literature.

Keywords: Resonant Tunneling Diode, Triangular Barrier, Quasi Energy States, Life Times.

1. Introduction

The development of sophisticated deposition techniques such as molecular beam epitaxy (MBE)[1] and metal-organic chemical vapor deposition techniques[2] made it possible to fabricate new materials based on ban-gap engineering with the required profiles and characteristics These technological man-made materials have enormous potential applications in high-speed and high-frequency devices[3-5] Resonant tunneling phenomena in heterostructure materials have been widely used for studying the quasiresonant tunneling energy states and their corresponding lifetimes for rectangle double-barrier structures using different techniques like variational method[6], Airy's function approach[7], transfer matrix approach[8-10], and for rectangle triple-barrier heterostructures[11-13] The effect of nonparabolicity on the resonant tunneling energies and resonant tunneling lifetimes of symmetric GaAs-Al$_x$Ga$_{1-x}$As rectangle double-barrier nanostructured has been reported[14,15] Recently, Elkenany and Elabsy[16] have addressed the effect of pressure on the resonant tunneling energy and resonant frequency tunneling on a rectangle double-barrier Ga$_{1-x}$Al$_x$As-GaAs nanostructure. It has been noticed that the structural properties of different profiles affect the electronic and physical properties of novel devices such as quantum rings[17,18], quantum dots[19-21], quantum wells[22-24], triangular double[25,26] and multi-barriers[27] Recently, triangular novel devices have a great considerable attention experimentally[28-32] and theoretically[25-27,33] than other devices due to their large uniformity, low cost, and high production yield[31] Most of the theoretical models rely on the transfer matrix method that determines the resonant tunneling energies from the peaks of the transmission coefficients data. In the mathematical manipulations of the triangular double-barrier the wavefunctions propagating through the triangular barrier were taken to be two separate solutions of the two types of Airy's functions one for each half of the triangle and applying the matching conditions at the bisector of the triangle and its base-vertices. In contrast, the current study employs a single wavefunction that travels through the barrier region of the triangle, and the complex-energy method is used to determine the quasi-resonant tunneling energies and their corresponding resonant tunneling lifetimes for an unbiased symmetric TDBN made up of GaAs-Al$_y$Ga$_{1-y}$As.

2. Theory

The present study uses atomic units, where m_0=e= $\hbar$=1 (unless otherwise stated).

Consider a symmetric TDBN composed of GaAs-Al$_y$Ga$_{1-y}$As as depicted in Fig. 1 of a potential energy barrier, V(z) in the form:

$$V(z) = \begin{cases} 0; & 0 \le |z| \le a \text{ and } |z| > a + 2b \\ \frac{V_0}{b}(z - a); & a < |z| \le a + b \\ \frac{V_0}{b}(a + 2b - z); & a + b < |z| \le a + 2b \end{cases} \quad (1)$$

Where a is the well half-width, b is the barrier half-thickness, V_0 is the barrier height, z is the direction of growth, and the potential energy barrier V(z) is an even function of z.
Solving Schrödinger equation for $|z| > 0$, one obtains even or odd bound state wavefunctions[34].

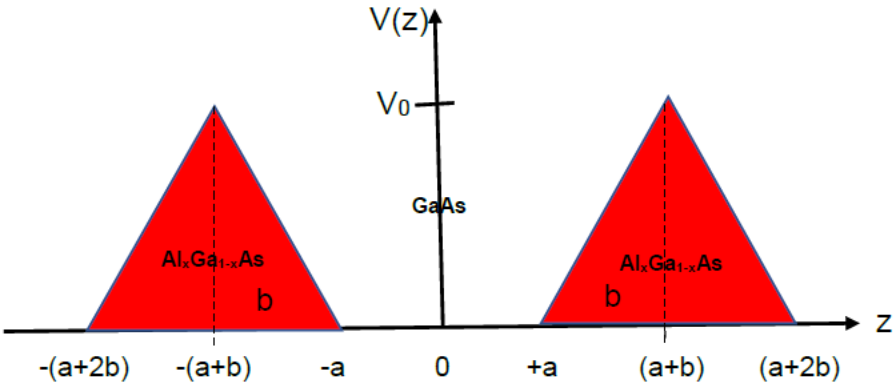

Figure 1: Symmetric triangular double-barrier nanostructure composed of GaAs-$Al_yGa_{1-y}As$ with a barrier height V_0, a well half-width, a, and a barrier half-thickness, b, with z-axis is taken as the growth direction.

2.1 Even Solution

The even wavefunction for the potential barrier given in eq. (1) in the (GaAs) well-region has the form:

$$\Psi(z) = A_1 \cos(kz)\,;\ 0 \le |z| \le a \quad (2)$$

where,

$$k = \sqrt{2\, m_1^*\, E_n}/\hbar \quad (3)$$

is the propagation wave vector in the GaAs region, A_1 is a coefficient, m_1^* is the electron effective mass in this region and E_n is the allowed energy states.
In the $Al_yGa_{1-y}As$ barrier-region, there are two independent solutions depends on the profile of the triangle:
i- The left hand side (LHS) region of the triangle or $a<|z| \le a+b$:
In this region, the time independent Schrödinger equation with m_2^* is the electron effective mass, is given by

$$\frac{d^2\Psi(z)}{dz^2} - \frac{2\, m_2^*}{\hbar^2}\left[\frac{V_0}{b}(z - a) - E_n\right]\Psi(z) = 0. \quad (4)$$

or,

$$\frac{d^2\Psi(z)}{dz^2} - \frac{2\, V_0\, m_2^*}{b\, \hbar^2}(z - \alpha_1)\Psi(z) = 0. \quad (5)$$

Where,

$$\alpha_1 = a + \frac{b\, E_n}{V_0} \quad (6)$$

One can rewrite eq. (5) in the form,

$$\frac{d^2\Psi(z)}{dz^2} - \beta_0\,(z - \alpha_1)\,\Psi(z) = 0. \quad (7)$$

Since

$$\beta_0 = \frac{2\,V_0\,m_2^*}{b\,\hbar^2} \tag{8}$$

Substitute with the parameter

$$\zeta = \beta\,(z - \alpha_1) \tag{9}$$

Then eq. (7) can be rewritten as

$$\frac{d^2\Psi(\zeta)}{d\zeta^2} - (\beta_0/\beta^3)\,\zeta\,\Psi(\zeta) = 0. \tag{10}$$

One can take β as

$$\beta = {\beta_0}^{1/3} = \left(\frac{2\,V_0\,m_2^*}{b\,\hbar^2}\right)^{1/3}. \tag{11}$$

By substituting the parameter β given in eq. (11) into eq. (10), one gets

$$\frac{d^2\Psi(\zeta)}{d\zeta^2} - \zeta\,\Psi(\zeta) = 0. \tag{12}$$

The above equation is the Airy's equation which has the outgoing solution

$$\Psi(\zeta) = A_2\,Ai(\zeta) \tag{13}$$

Where,

$$\zeta = \left(\frac{2\,V_0\,m_2^*}{b\,\hbar^2}\right)^{\frac{1}{3}}(z - \alpha_1), \tag{14}$$

and A_2 is a coefficient.

ii- The right hand side (RHS) region of the triangle or $a+b<|z|\leq a+2b$:

In this region, the time independent Schrödinger equation with m_2^* is the electron effective mass, is given by

$$\frac{d^2\Psi(z)}{dz^2} - \frac{2\,m_2^*}{\hbar^2}\left[\frac{V_0}{b}(a + 2b - z) - E_n\right]\Psi(z) = 0. \tag{15}$$

Rewrite (15) to be in the form,

$$\frac{d^2\Psi(z)}{dz^2} + \beta_0\,(z + \alpha_2)\Psi(z) = 0. \tag{16}$$

Where,

$$\alpha_2 = \frac{b\,E_n}{V_0} - (a + 2b) \tag{17}$$

Substitute into eq. (16) by the parameter,

$$\eta = -\,\beta\,(z + \alpha_2) \tag{18}$$

Where, η is an unknown parameter to be determined, then eq. (16) can take the form,

$$\frac{d^2\Psi(\eta)}{d\eta^2} - (\beta_0\,/\beta^3)\,\eta\,\Psi(\eta) = 0 \tag{19}$$

Similarly, as before eq. (19) can be rewritten in the form of Airy's equation as

$$\frac{d^2\Psi(\eta)}{d\eta^2} - \eta\,\Psi(\eta) = 0 \tag{20}$$

Where, the parameter β is the same as given in eq. (11), and η is a function of z takes the expression,

$$\eta(z) = -\left(\frac{2\,V_0\,m_2^*}{b\,\hbar^2}\right)^{\frac{1}{3}}\left[z + \frac{b\,E_n}{V_0} - (a+b)\right] \tag{21}$$

The solution of eq. (20) can be taken as

$$\Psi[\eta(z)] = A_3\,Ai[\eta(z)] \tag{22}$$

The general solution of the wavefunction inside the triangular barrier region can be taken as a combination of the solutions of the two equations given in equations (13) and (22) as

$$\Psi(z) = A_2\,Ai[\zeta(z)] + A_3\,Ai[\eta(z)] \tag{23}$$

The above choice of the wavefunction inside the triangular barrier region is considered to ensure that it satisfies the concepts of quantum Physics that wavefunction must be continuous and single valued. The coefficients A_2 *and* A_3 can be determined from the continuity conditions of the wavefunctions and their slopes at the boundaries of the triangle.

The detector region behind the triangle i.e., $|z|>a+2b$:

Solving Schrödinger equation in this region where V(z) = 0 is an outgoing plane wave in the form

$$\Psi(z) = A_4\,e^{ikz} \tag{24}$$

Where A_4 is the transmission coefficient and k is a propagation vector as given in eq. (2).
To guarantee a current conservation at the boundaries of the triangle, the wavefunctions $\Psi(z)$ and their derivatives $1/m_i^*\,d\Psi(z)/dz$ (i=1 *or* 2) in which i=1 stands for well-GaAs and i=2 stands for barrier-$Al_yGa_{1-y}As$ layers; respectively must be continuous at the boundaries: z=a+(b/2) and z=a+(3b/2) at these points $V(z)=V_0/2$.

After algebraic manipulation one obtains a transcendental equation for the allowed quasi-resonant tunneling even-energy eigenvalues of the form:

$$tan(c_3) = \frac{1}{\delta}\left[\frac{-R_1\cdot A_i'(c_1) + R_2\cdot A_i'(c_2)}{R_1\cdot A_i(c_1) + R_2\cdot A_i(c_2)}\right] \tag{25}$$

Where,

$$\delta = k\gamma/\beta, \tag{26}$$

$$R_1 = i\delta A_i(c_1) + Ai'(c_1) \tag{27a}$$

$$R_2 = -i\delta A_i(c_2) + Ai'(c_2) \tag{27b}$$

$$c_1 = \beta\left(\frac{b}{2} - \alpha_0\right);\ \alpha_0 = b\,E_n/V_0 \tag{28}$$

$$c_2 = \beta\left(\frac{3\,b}{2} - \alpha_0\right) \tag{29}$$

2.2 Odd Solution

The odd wavefunctions for the potential energy barrier given in eq. (1) can be taken as

$$\Psi(z) = A_5 \sin(kz)\,;\ 0 \le |z| \le a \tag{30}$$

Where A_5 is the incident coefficient and k is the propagation wave vector as given in eq. (3).

The solutions of Schrödinger equation in the triangular barrier-$Al_yGa_{1-y}As$ layer will be the same as those given in equations (13) and (22).

Similarly, the solution in the detector region will be the same as given by eq. (24). Applying the matching conditions of the wavefunctions and considering the odd solution of eq. (31) at the boundaries z=a+(b/2) and z=a+(3b/2), one obtains a transcendental equation for the allowed quasi-resonant tunneling odd-energy eigenvalues of the form,

$$cot(c_3) = -\frac{1}{\delta}\left[\frac{-R_1 \cdot A_i'(c_1) + R_2 \cdot A_i'(c_2)}{R_1 \cdot A_i(c_1) + R_2 \cdot A_i(c_2)}\right] \tag{31}$$

Solving the transcendental eq. (25), one gets the allowed quasi-resonant tunneling even energy states E_n (n = 1, 3, 5, …) and the allowed quasiresonant tunneling odd energy ($excited$) states E_n (n = 2, 4, 6, …) by solving eq. (31), since (n = 1) is related to the lowest (ground) even-energy state.

The roots of equations (25) and (31) as functions of V_0, a, and b were computed numerically by using MATLAB language[35]. It is noticed that all roots were complex values with negative imaginary parts[8].

The concepts of quasi-resonant tunneling stationary energy states is introduced for tunneling mechanism[36]. The real part of the root is corresponding to the quasi-resonant tunneling energy while the imaginary counterpart is assigned to the quasi-resonant tunneling lifetime involving the energy-time uncertainty relationship $\varepsilon_n \sim 1/\tau_n$ as follows:

$$E_n = Real\ (\Gamma_n) \tag{32}$$

Where Γ_n is the n^{th} – root of the transcendental equations.

$$\mathrm{n} = \begin{cases} 1, 3, 5, \ldots & for\ even\ energy\ states \\ 2, 4, 6, \ldots & for\ odd\ energy\ states \end{cases} \tag{33}$$

$$\varepsilon_n = Imag\ (\Gamma_n) \tag{34}$$

Since the total energy,

$$\Gamma_n = E_n - i\ \varepsilon_n/2 \tag{35}$$

is the solution of the time dependent Schrödinger equation,

$$\Psi_n(z,t) = \Psi_n(z).e^{-i\,\Gamma_n t} = \Psi_n(z).e^{-i\,E_n - \varepsilon_n t/2} \tag{36}$$

The probability density of eq. (36) gives,

$$|\Psi_n(z,t)|^2 = |\Psi_n(z)|^2 .e^{-\varepsilon_n t} \tag{37}$$

It is seen from eq. (37) that the probability density decreases with time as $e^{-\varepsilon_n t}$, then the lifetime of the n^{th} resonant tunneling energy state has the form,

$$\tau_n = -\frac{1}{\varepsilon_n/2} = -\frac{2}{\varepsilon_n}(\mathrm{sec}) \tag{38}$$

3. Results

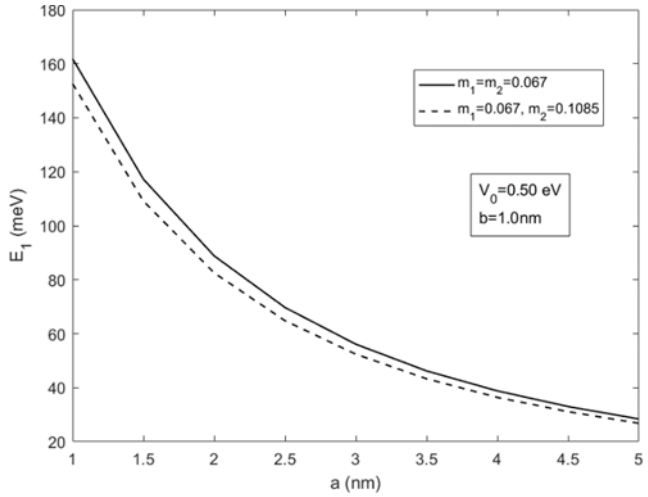

Figure 2: Variation of the resonant tunneling lowest energy, E_1, given in meV with the well half-width, a, for a TDBN of GaAs-$Al_yGa_{1-y}As$ at V_0=0.50 eV, a=2.5 nm, b=1.0 nm and different effective masses of m_1^* =0.067 and m_2^* =0.1085.

Figure 2 shows the dependence of the lowest resonance tunneling energy E1 on the half well width, a, for the GaAs-$Al_yGa_{1-y}As$ TDBN with a barrier height of 0.50 eV and different effective electron masses within the well and barrier regions. The decreasing tendency in the lowest energy with increasing width is in accordance with the principles of quantum physics[36]. It is also seen the pronounced discrepancy between the same masses and the mass mismatch condition which is very important when studying hetero nanostructures. By comparing the resonant tunneling energies of the present study with those of Ref.[27], we found good agreement as seen in Table 1.

Table 1 also presents the associated lifetimes τ_1 and τ_2 in fs.

E_1 (meV)		E_2 (meV)		τ_1 (fs)	τ_2 (fs)
P.W. [eq. 25]	Ref.[27]	P.W. [eq. 31]	Ref.[27]	P.W. [eq. 38]	P.W. [eq. 38]
64.8	65.5	293.6	298.6	43.78	8.17

Table 1: Comparison between the resonant tunneling lowest, E_1, and first excited, E_2, energies given in meV and their associated resonant tunneling lifetimes τ_1 and τ_2 given in fs, for a TDBN of GaAs-$Al_yGa_{1-y}As$ with m_1^* =0.067 a.u, m_2^* =0.1085, a=2.5 nm, b=1.0 nm and V_0=0.50 eV.

It must be mentioned that the present study performed the computations for well half-width, in contrast with the other published data in which the well full width was used.

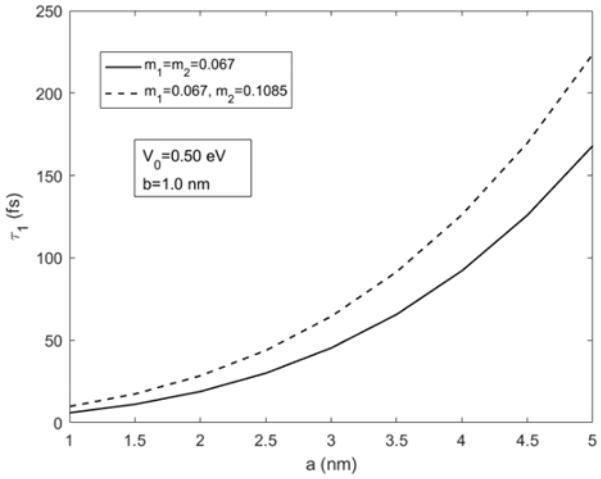

Figure 3: Variation of the resonant tunneling lowest lifetime, τ_1, given in fs, with the well half-width, a, for a TDBN of GaAs-$Al_yGa_{1-y}As$ at V_0=0.50 eV, a=2.5 nm, b=1.0 nm and different effective masses of m_1^* =0.067 and m_2^* =0.1085.

Figure 3 presents the dependence of the resonant tunneling lowest

lifetime, τ_1, upon the well half-width, a, at a barrier height of 0.50 eV, a barrier half-thickness of 1.0 nm, and different electron effective masses interior to the well and the barrier regions. In Fig. 3 the increase in the resonant tunneling time by expanding the well width is in accordance with the physical concept that widening the well diminishes the resonant energy and subsequently increases the tunneling time of electrons.

Figure 4 depicts the dependence of the quasi-resonant tunneling energies for both lowest, E_1 and first excited, E_2 energy states on the aluminum concentration, y at constant well half-width of 2.5 nm and barrier halfthickness of 1.0 nm for considering the electron's effective mass mismatch condition, $m_2^*=m_2^*(y)$ and ignoring it, $m_2^* =m_1^*=0.067$.

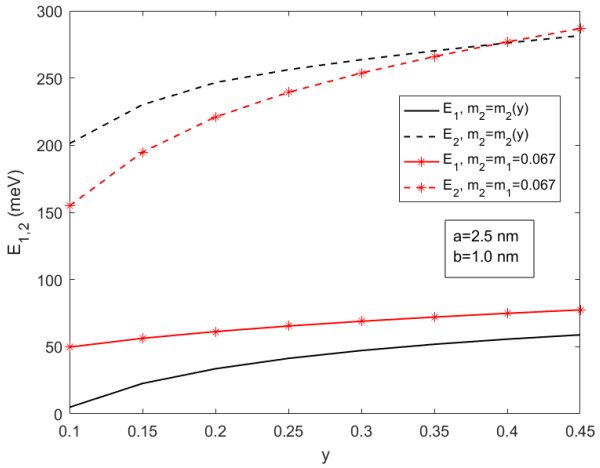

Figure 4: Variation of the resonant tunneling lowest, E_1 (solid curves) and first excited, E_2 (dashed curves) energies given in meV with the aluminum concentration, y, for a TDBN of GaAs-$Al_yGa_{1-y}As$ at constant a=2.5 nm and b=1.0 nm for mass mismatch (black curves) and same masses (red curves).

The enhancement of both quasi-resonant energies by increasing the aluminum mole fraction (concentration), y in the barrier region illustrated in Fig. 4, is dependent on the rise in y which leads to an increase in the barrier height, V_0 and in turn, increases the quasi-resonant energy.

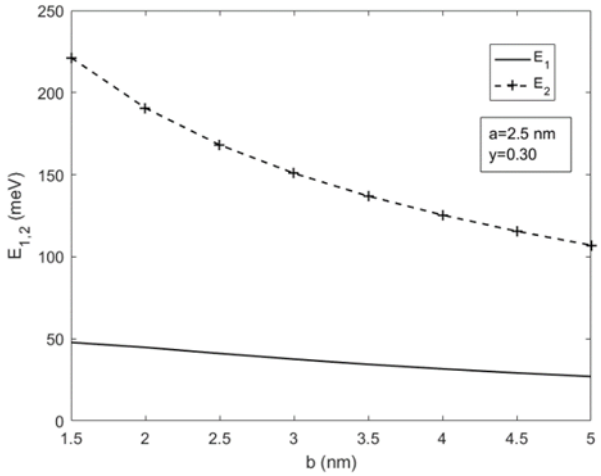

Figure 5: Variation of the quasi-resonant tunneling lowest, E_1 (solid curve) and first excited, E_2 (dashed curve) energies given in meV with the barrier half-thickness, b (nm) for a TDBN of GaAs-$Al_yGa_{1-y}As$ at constant aluminum concentration, y=0.30, well half-width a=2.5 nm.

Figure 5 exhibits the variation of the quasi-resonant tunneling energies for lowest, E_1 and first excited states, E_2 as functions of the barrier halfthickness, b for a TDBN of GaAs-$Al_yGa_{1-y}As$ at a constant aluminum concentration (content), y = 0.30 and well half-width a = 2.5 nm. Both quasiresonant tunneling energies decrease as the barrier becomes thicker which in turn lowers the quasi-resonant tunneling energies.

Figure 6 illustrates the dependence of the quasi-resonant tunneling lifetimes of the lowest state, τ_1 and the first excited state. τ_2 on the halfthickness of the barrier, b for a TDBN composed of GaAs-$Al_yGa_{1-y}As$ at fixed aluminum concentration, y of 0.30,

and well half-width, a of 2.5 nm. It is observed that as the barrier thickness increased, the quasi-resonant tunneling lifetimes for both states also increased, resulting in an enhancement of the quasi-resonant tunneling lifetimes. The exponential tendency of increasing lifetimes means that the full energy bandwidth of resonant energy peak at half maximum becomes smaller and the wavefunction is sharper. The results of the present study are in good agreement with the experimental data[37] that the tunneling time through a barrier amounted to 1.0 ps.

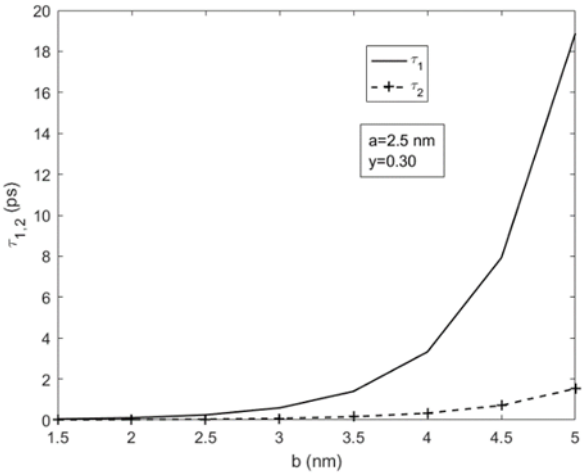

Figure 6: Variation of the quasi-resonant tunneling lifetimes for lowest, τ_1 (solid curve) and first excited states, τ_2 (dashed curve) given in ps with the barrier half-thickness, b (nm) for a TDBN of GaAs-$Al_yGa_{1-y}As$ at fixed aluminum concentration, y=0.30 and well half-width a=2.5 nm.

4. Conclusion

This study utilizes the complex energy method, where the roots of the transcendental equations for resonant tunneling energy states, both even and odd, are complex. The real part is attributed to the quasi-resonant tunneling energy state, while the imaginary part is linked to the quasiresonant tunneling lifetime, in accordance with the energy-time uncertainty principle. The computed resonant tunneling energies and lifetimes of the P.W. were compared to the relevant published data, and the results showed excellent agreement. This study highlights the significant impact of mass mismatch on the computation of quasi-resonant tunneling energies and their associated lifetimes in hetero-nanostructure devices. In addition, the physical properties of the nanostructure materials can be adjusted to regulate the performance of their devices.

Data Availability: The data that support the findings of this study are available from the corresponding author on reasonable request. No restrictions apply.

Conflicts of Interest: The authors declare no competing interests.

Online Content: Any methods, additional references, Nature Research reporting summaries, source data, statements of code and data availability and associated accession codes are available.

Funding: This research did not receive any specific grant from funding agencies in the public, commercial, or not-for-profit sectors.

References

1. Wasa, K. (2012). Sputtering phenomena. Handbook of Sputtering Technology, 41-75.
2. Ludowise, M. J. (1985). Metalorganic chemical vapor deposition of III-V semiconductors. Journal of Applied Physics, 58(8), R31-R55.
3. Li, H., Chang, C. J., Kuo, S. Y., Wu, H. C., Huang, H., & Lu, T. C. (2018). Improved performance of near UV GaN-based light emitting diodes with asymmetric triangular multiple quantum wells. IEEE Journal of Quantum Electronics, 55(1), 1-4.
4. Kudrawiec, R., & Hommel, D. (2020). Bandgap engineering in III-nitrides with boron and group V elements: Toward applications in ultraviolet emitters. Applied Physics Reviews, 7(4).
5. Shakoury, R., Arman, A., Ţălu, Ş., Dastan, D., Luna, C., & Rezaee, S. (2020). Stereometric analysis of TiO2 thin films deposited by electron beam ion assisted. Optical and Quantum Electronics, 52(5), 270.
6. Bastard, G., Mendez, E. E., Chang, L. L., & Esaki, L. (1983). Variational calculations on a quantum well in an electric field. Physical Review B, 28(6), 3241.
7. Vatannia, S., & Gildenblat, G. (1996). Airy's functions implementation of the transfer-matrix method for resonant tunneling in variably spaced finite superlattices. IEEE Journal of Quantum Electronics, 32(6), 1093-1105.
8. Elkenany, E. B., & Elabsy, A. M. (2022). Comparative investigation between complex energy and transfer matrix techniques for quasi-energy states in heterostructure materials. Journal of Materials Science: Materials in Electronics, 33(28), 22469-22479.
9. Mukherjee, K., & Das, N. R. (2009, December). Calculation of current in multiple quantum well structure with variable barrier heights. In 2009 4th International Conference on Computers and Devices for Communication (CODEC) (pp.

1-4). IEEE.
10. Jonsson, B., & Eng, S. T. (1990). Solving the Schrodinger equation in arbitrary quantum-well potential profiles using the transfer matrix method. IEEE journal of quantum electronics, 26(11), 2025-2035.
11. Talele, K., & Patil, D. (2008). Analysis of wave function, energy and transmission coefficients in GaN/AlGaN superlattice nanostructures. Progress In Electromagnetics Research, 81, 237-252.
12. Zarifkar, A., & Bagherabadi, A. M. (2008). Numerical Analysis of Triple–Barrier GaAs/$Al_yGa_{1-y}As$ Resonant Tunneling Structure Using PMM Approach. IJCSNS, 8(6), 266.
13. Xu, J., Schubert, M. F., Noemaun, A. N., Zhu, D., Kim, J. K., Schubert, E. F., & Park, Y. (2009). Reduction in efficiency droop, forward voltage, ideality factor, and wavelength shift in polarization-matched GaInN/GaInN multi-quantum-well light-emitting diodes. Applied Physics Letters, 94(1).
14. Elabsy, A. M., & Elkenany, E. B. (2022). Effect of the nonparabolicity on the resonant lifetimes and resonant energies of symmetric GaAs/AlxGa1-xAs double barrier nanostructures. Physica B: Condensed Matter, 632, 413711.
15. Tomić, S., O'Reilly, E. P., Klar, P. J., Grüning, H., Heimbrodt, W., Chen, W. M., & Buyanova, I. A. (2004). Influence of conduction-band nonparabolicity on electron confinement and effective mass in $GaN_x As_{1-x}$/GaAs quantum wells. Physical Review B, 69(24), 245305.
16. Elkenany, E. B., & Elabsy, A. M. (2022). Impact of pressure on the resonant energy and resonant frequency for two barriers $Ga_{1-x}Al_xAs$/GaAs nanostructures. Physica Scripta, 98(1), 015809.
17. Hernández, N., López, R., Álvarez, J. A., Marín, J. H., Fulla, M. R., & Tobón, H. (2021). Optical absorption computation of a D2+ artificial molecule in GaAs/Ga1−xAlxAs nanometer-scale rings. Optik, 245, 167637.
18. Vinasco, J. A., Radu, A., Niculescu, E., Mora-Ramos, M. E., Feddi, E., Tulupenko, V., & Duque, C. A. (2019). Electronic states in GaAs-(Al, Ga) As eccentric quantum rings under nonresonant intense laser and magnetic fields. Scientific Reports, 9(1), 1427.
19. Heyn, C., Radu, A., Vinasco, J. A., Laroze, D., Restrepo, R. L., Tulupenko, V., & Duque, C. A. (2021). Exciton states in conical quantum dots under applied electric and magnetic fields. Optics & Laser Technology, 139, 106953.
20. Mommadi, O., El Moussaouy, A., Chnafi, M., El Hadi, M., Nougaoui, A., & Magrez, H. (2020). Exciton–phonon properties in cylindrical quantum dot with parabolic confinement potential under electric field. Physica E: Low-dimensional Systems and Nanostructures, 118, 113903.
21. Bera, A., & Ghosh, M. (2017). Simultaneous influence of hydrostatic pressure and temperature on binding energy of impurity doped quantum dots in presence of noise. Journal of Alloys and Compounds, 695, 3054-3060.
22. Elabsy, A. M. (1993). Hydrostatic pressure dependence of binding energies for donors in quantum well heterostructures. Physica Scripta, 48(3), 376.
23. Elabsy, A. M. (2000). Effective mass dependence of resonant quasi-level lifetime in GaAs–$Al_xGa_{1-x}As$ double-barrier structures. Physica B: Condensed Matter, 292(3-4), 233-237.
24. Kasapoglu, E. S. İ. N. (2008). The hydrostatic pressure and temperature effects on donor impurities in GaAs/Ga1−xAlxAs double quantum well under the external fields. Physics Letters A, 373(1), 140-143.
25. Wang, H., Xu, H., & Zhang, Y. (2006). A theoretical study of resonant tunneling characteristics in triangular double-barrier diodes. Physics Letters A, 355(6), 481-488.
26. Ohmukai, M. (2005). Triangular double barrier resonant tunneling. Materials Science and Engineering: B, 116(1), 87-90.
27. Luo, M., Yu, G., & Xia, L. (2015). Calculation of conductance for triangular multi-barrier structure in a constant electric field. Superlattices and Microstructures, 83, 168-175.
28. Li, G., Song, W., Wang, H., Luo, X., Luo, X., & Li, S. (2018). Performance improvement of UV light-emitting diodes with triangular quantum barriers. IEEE Photonics Technology Letters, 30(12), 1071-1074.
29. Kim, J. Y., Kwon, M. K., Kim, J. P., & Park, S. J. (2007). Enhanced light extraction from triangular GaN-based light-emitting diodes. IEEE Photonics Technology Letters, 19(23), 1865-1867.
30. Li, H., Chang, C. J., Kuo, S. Y., Wu, H. C., Huang, H., & Lu, T. C. (2018). Improved performance of near UV GaN-based light emitting diodes with asymmetric triangular multiple quantum wells. IEEE Journal of Quantum Electronics, 55(1), 1-4.
31. Guzmán, A., Sánchez-Rojas, J. L., Tijero, J. M. G., Hernando, J., Calleja, E., Muñoz, E., & Montojo, M. T. (1999). Growth and characterization of a bound-to-quasi-continuum QWIP with Al-graded triangular confinement barriers. IEEE Photonics Technology Letters, 11(12), 1650-1652.
32. Elpelt, R., Wolst, O., Willenberg, H., Malzer, S., & Döhler, G. H. (2004). Electron transport through triangular potential barriers with doping-induced disorder. Physical Review B, 69(20), 205305.
33. Ohmukai, M. (2003). The gradient of the barriers affects the resonant energy. Modern Physics Letters B, 17(09), 383-386.
34. Morrison, M. A. (1990). Understanding Quantum Physics. Prentice-Hall, Inc.
35. Gilat, A., MATLAB. (2005). An Introduction with Application. 2nd Edit., John Wiley & Sons, Inc.
36. Landau, L. D., Lifshitz, E. M. (1977). Quantum Mechanics. Pergamon, N.Y.
37. Schubert, E. F., Cunningham, J. E., & Tsang, W. T. (1987). Realization of the Esaki-Tsu-type doping superlattice. Physical Review B, 36(2), 1348.